ACS Photonics

Letter

pubs.acs.org/journal/apchd5

Shaping Photoluminescence Spectra with Magnetoelectric Resonances in All-Dielectric Nanoparticles

Isabelle Staude,*[,†,‡] Vyacheslav V. Khardikov,[⊥,§] Nche T. Fofang,[‡] Sheng Liu,[‡] Manuel Decker,[†] Dragomir N. Neshev,[†] Ting Shan Luk,[‡] Igal Brener,[‡] and Yuri S. Kivshar[†]

[†]Nonlinear Physics Centre and Centre for Ultra-high bandwidth Devices for Optical Systems (CUDOS), Research School of Physics and Engineering, The Australian National University, Canberra, ACT 2601, Australia

[‡]Center for Integrated Nanotechnologies, Sandia National Laboratories, Albuquerque, New Mexico 87185, United States

[⊥]V.N. Karazin Kharkiv National University, Kharkiv 61022, Ukraine

[§]Institute of Radio Astronomy, National Academy of Sciences of Ukraine, Kharkiv 61002, Ukraine

S *Supporting Information*

ABSTRACT: We measure the near-infrared photoluminescence spectra of colloidal quantum dots coupled to the localized electric and magnetic resonances of subwavelength silicon nanodisks. The spectral position of the resonances with respect to each other is controlled via the nanodisk geometry. We observe a strong influence of the nanodisk resonance positions on the quantum dot photoluminescence spectra. For separate resonances, the spectral density observed in transmittance measurements correlates with the spectral range covered by a broad emission spectrum. For the case of spectral overlap of the electric and magnetic dipolar resonances we enter a new regime for coupling, where the characteristic transparency effect evident in the transmittance spectra is accompanied by a pronounced single emission maximum. Our experimental observations are in good qualitative agreement with numerical calculations.

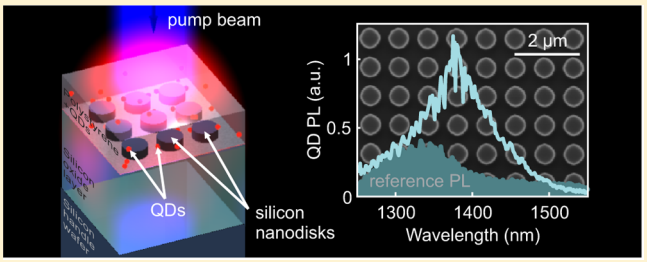

KEYWORDS: *nanoantennas, quantum light sources, all-dielectric nanophotonics, magnetic resonance, light scattering, quantum dots*

Owing to their numerous potential applications such as efficient quantum light sources, biosensing, and efficiency-enhanced solar cells, optical nanoantennas have become an active field of research.[1,2] Up to now, research into optical nanoantennas has been mostly focused on plasmonic structures, due to the large field enhancements[3] that can be achieved in plasmonic hot spots. However, the performance of plasmonic nanoantennas is compromised by strong dissipative losses of metals at optical frequencies. This is particularly critical for complex nanoantennas comprising larger amounts of metal, such as arrayed nanoantennas for unidirectional scattering,[4,5] and for nanoantennas that rely on loss-sensitive effects. Examples of the latter include magnetic Fano resonances[6−8] or on-demand emission of single or entangled photons.[9,10] Furthermore, the strong losses also imply that the quantum efficiency of a hybrid system consisting of an already efficient nanoemitter coupled to a plasmonic particle will be significantly lower than that of the nanoemitter alone in many cases, as the fraction of the energy going into nonradiative channels is usually increased by the presence of a lossy metallic structure.[11] It is worth noting that this drawback is not obvious from the most commonly specified characteristics of plasmonic nanoantennas, namely, directivity, beam width, and front-to-back ratio, which merely describe the emission pattern, but do not take the radiation efficiency of the nanoantenna into account.

A possible way to overcome the problem of dissipative losses in plasmonic nanoantennas is to rely on low-loss dielectric designs, which utilize the localized modes of high-index dielectric (e.g., silicon) nanoparticles. Considerable efforts have been made recently to understand the modes and scattering properties of such high-index all-dielectric subwavelength nanoparticles, revealing that they support both electric and magnetic diplar resonances.[12−16] Importantly, by reducing the symmetry of the nanoparticles, e.g., using nanodisks as opposed to the widely studied spheres, it is possible to tune the spectral positions of their fundamental electric and magnetic modes with respect to each other through a simple variation of the disk aspect ratio, including the important case of overlapping both these resonances at the same spectral position.[16]

Furthermore, all-dielectric nanoparticles,[17,18] nanoantenna arrays,[19] and metamaterials[20] have already been theoretically studied for light extraction and emission enhancement applications. Recent work predicts that such dielectric nanoparticles can perform as highly directional nanoantennas[16,21−23]

Received: October 13, 2014
Published: January 15, 2015

DOI: 10.1021/ph500379p
ACS Photonics 2015, 2, 172−177

and that even for single-element all-dielectric nanoantennas huge front-to-back ratios in combination with high directivities can be obtained.[16] Of particular interest is the role of the magnetic resonances, as they provide a novel additional channel for influencing emission dynamics. In fact, the formation of magnetic field hot-spots can be expected for high-index all-dielectric nanoparticles, suggesting dielectric nanoantennas as a promising platform for controlling magnetic dipolar emission.[24,25] Experimentally, however, the use of all-dielectric nanoparticles supporting electric and magnetic resonances as photonic elements for tailoring the emission of nanoemitters remains unexplored. Here we demonstrate, for the first time to our knowledge, the coupling of quantum dots (QDs) to such resonant silicon nanoparticles and investigate the emission properties of the coupled system. In particular, we demonstrate that for the condition of the spectral overlap of electric and magnetic resonances of comparable strength, which is a unique property of our system, we achieve an emission spectrum exhibiting a single maximum. In contrast to the case of separate resonances, this maximum is not accompanied by a corresponding resonant feature in the transmittance spectrum. We note that this is a new coupling regime never attained with plasmonic nanoparticles to date. While a range of interesting effects including modifications of the emission spectrum,[26−29] strong Purcell enhancement,[28,30] directional emission,[4,31] polarization-engineered emission,[29,31] and excitation enhancement[32] have been demonstrated for plasmonic particles, the overlap of electric and magnetic resonances of comparable strength is not possible with a single metallic nanoparticle. Recent studies[29] have attempted the regime of overlapping resonances with electric and magnetic dipole contributions; however the emission in each mode has been studied separately for two orthogonal polarizations. Our system, in contrast, is characterized by electric and magnetic dipole modes that can be excited simultaneously by the same polarization and shows no polarization dependence.

A schematic drawing of our experimental geometry is shown in Figure 1a. We consider arrays of silicon disks as all-dielectric nanoantennas featuring a systematic variation of the disk aspect ratio. Silicon is a particularly attractive material choice because it not only provides a sufficiently large refractive index to support magnetic modes while exhibiting extremely low losses in the near-infrared (NIR) spectral range but also is fully compatible with standard electronics and microphotonics.

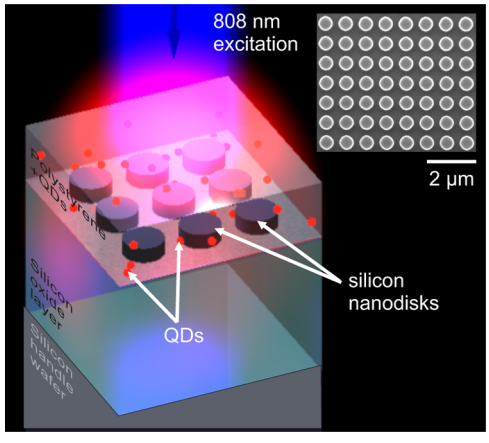

Figure 1. Sketch of the sample geometry (not to scale). The inset shows a scanning electron micrograph of a typical silicon nanodisk sample.

We fabricated silicon disks on silicon oxide using electron-beam lithography (EBL) on silicon-on-insulator wafers. A scanning electron micrograph of a typical silicon nanodisk sample is displayed in the inset of Figure 1. The samples were then spin-coated with a polystyrene layer containing PbS QDs emitting in the near-infrared spectral range, which resulted in the silicon disks being embedded inside the QD-PS matrix as schematically depicted in Figure 1. Details of the fabrication procedure can be found in the Methods section.

As a next step, we measured the linear-optical transmittance spectra for arrays of silicon nanodisks with different nanodisk diameters embedded into the QD-PS matrix (see Methods for details). These results are depicted in Figure 2a. The sample

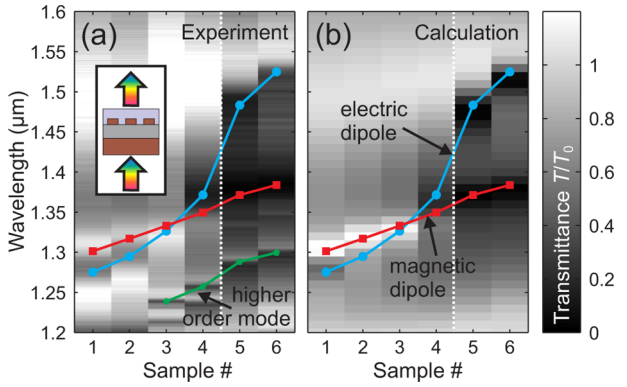

Figure 2. (a) Experimentally measured linear-optical relative transmittance spectra T/T_0 of silicon nanodisks with varied disk diameter covered by a layer of QD-containing polystyrene and (b) corresponding numerically calculated transmittance spectra. The solid lines are guides to the eye, showing the individually calculated electric (cyan) and magnetic (red) mode positions. The additional green line in (a) indicates the approximate position of the higher-order mode that appears in experimental spectra due to not strictly normal incidence. The sample numbers 1−6 correspond to nanodisk diameters of 425, 450, 475, 500, 575, and 600 nm, respectively. The inset in (a) shows a schematic of the illumination scenario used in transmittance measurements. The white dashed lines mark a larger increment in the nanodisk radii.

numbers 1−6 correspond to nanodisk diameters of 425, 450, 475, 500, 575, and 600 nm, respectively, which were determined by taking size estimates from scanning electron micrographs and varying the diameter in numerical simulations until finding the best fit for the corresponding measured resonance positions before the application of the QD-containing layer. This procedure allows compensating for slightly inclined sidewalls, which cause the nanodisks to appear slightly smaller in optical measurements as compared to top-view SEM images.[33] For all samples the center-to-center distance between neighboring nanodisks was a = 800 nm. Each fabricated array has a footprint of 500 μm × 500 μm.

In order to compare the measured transmittance spectra with theory, we performed numerical frequency domain simulations using CST Microwave Studio with unit-cell boundary conditions. Figure 2b shows calculated normal-incidence transmittance spectra for arrays of silicon nanodisks with the dimensions given above, where we have taken into account the silicon oxide layer, the silicon handle wafer, and the experimental referencing procedure. We used n_{SiO_x} = 1.45 for

DOI: 10.1021/ph500379p
ACS Photonics 2015, 2, 172−177

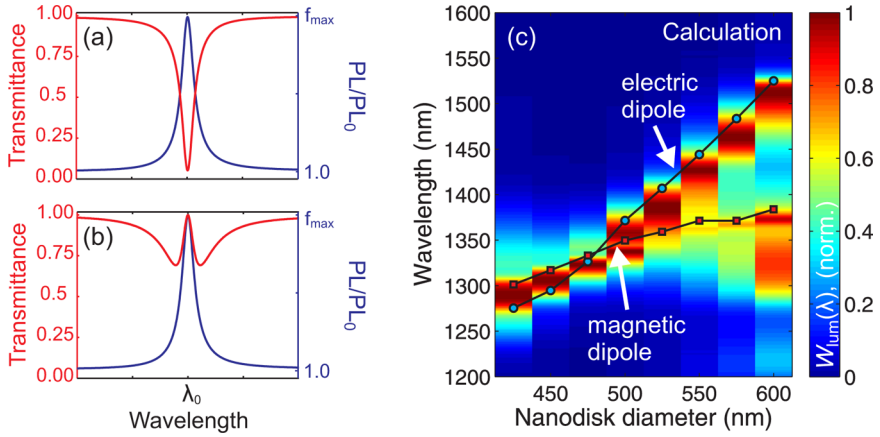

Figure 3. Schematic of typical transmittance line shapes and corresponding expected QD PL line shape variations for (a) an individual optical resonance and (b) overlapping electric and magnetic resonances. f_{max} denotes the maximum PL enhancement factor. Far-field interference of an incident plane wave and the light scattered by the electric and magnetic resonances leads to a transparency effect in transmittance for the resonance overlap. For electric and magnetic resonances having nonidentical widths and/or strengths a characteristic Fano-feature is observed in transmittance spectra.[34] (c) Normalized numerically calculated emission spectra of the hybrid system for a variation of the nanodisk diameters when modeling the QD-containing layer as a homogeneous medium with frequency-dependent gain. The solid lines show separately calculated spectral positions of the electric and magnetic dipole modes from CST simulations.

the silicon oxide layer and $n_{Si} = 3.5$ for the silicon disks and the handle wafer. The QD-containing polystyrene layer is modeled as a flat film with a thickness of $h_{PS} = 250$ nm and an effective refractive index $n_{PS} = 1.46$, which was chosen to reproduce the experimentally observed red-shift of the resonances after the application of the layer. The height of the silicon nanodisks is fixed to $h = 220$ nm. Also shown are the independently calculated spectral positions of the nanodisks' fundamental electric and magnetic dipole resonance positions obtained from electric and magnetic field probes located at the center of the nanodisks, respectively, under plane-wave excitation.[16]

Good agreement is obtained between the experimental and the theoretical transmittance curves. In particular, for the sample with $d = 600$ nm (sample #6) we observe two separate resonances, namely, the fundamental electric resonance of the nanodisks around 1515 nm and the fundamental magnetic resonance around 1375 nm. As the disk diameter is decreased, the two resonances move closer together and start merging for $d = 500$ nm (sample #4, note that the nanodisk diameter increment is larger between samples #4 and #5). For a further reduction of the diameter, leading to an overlap of the electric and magnetic resonances, the structure becomes more transparant as a result of resonant forward scattering as discussed in refs 16 and 34. In our experiment this effect is most pronounced for $d = 475$ nm (sample #3). As the diameter is decreased even further, the mode signature in the transmittance spectra starts to get more pronounced again. The slight deviations between experiment and theory are mainly caused by sample imperfections such as roughness and deviations from the perfect disk shape. The additional transmittance minima present in the experimental curves at the short-wavelength side of the resonances can be attributed to higher-order modes that can be excited due to the finite numerical aperture in the experiment.

Next we study the emission of QDs coupled to these resonant silicon nanoparticles. It is well known that the decay rate of a quantum emitter placed in close proximity to a nanoantenna will be modified due to the modified local density of states available for the decay of the system, compared to the case of a homogeneous medium.[2] For plasmonic particles coupled to emitters, the partial local density of states (LDOS) and, hence, the resulting radiation spectrum of the emitters can be linked to the absorption spectra of the plasmonic particles.[28,29] For the case of all-dielectric resonant nanoparticles, where the absorption is negligible, we can usually resort to the resonance dips in the transmission spectra as an indication for resonant enhancement of the number of photonic end states available for radiative decay. This picture allows us to make qualitative predictions about the emission spectra as schematically illustrated in Figure 3a. The dips in transmittance originate from the extinction of the incident wave due to resonant scattering by the silicon nanodisks.[16] However, at the position of overlap of the electric and magnetic resonances, the resonance signatures disappear and the transmission dips are not centered at the position of the resonances anymore (see Figure 3b). In other words, the transmittance spectra can no longer be used to obtain information about the partial LDOS, raising the important question of how the emission spectra will be modified by the presence of such magneto-electric resonant nanoparticles. To answer this question, we recall that the partial LDOS is enhanced at the position of the resonances and that the observation of transmittance minima for separate resonances is just a secondary effect. Here, for the case of resonance overlap, while the structure becomes more transparent due to the strong forward scattering[16] and transmittance can even become unity,[34] the partial LDOS at the spectral overlap position is the sum of the partial LDOS of the two resonances. On the basis of our understanding of the resonance properties of the silicon nanodisks we can therefore expect that the PL spectra of emitters coupled to such all-dielectric nanoparticles will show a single local maximum, which is in contrast to the characteristic Fano-feature, which may be expected from the transmittance spectra (see Figure 3b).

In order to provide a theoretical estimate of such spectral line shaping in a coupled system of an emitter and magneto-electric resonant nanoparticle, we resort to the method proposed in ref 20 and evaluate $W_{lum} \approx -W_g$, where W_g is the (negative) dissipation intensity in our structure with a frequency-dependent gain assigned to the QD layer (see Supporting

DOI: 10.1021/ph500379p
ACS Photonics 2015, 2, 172−177

Information for details). While quantitative results for a gain structure and for a system dominated by spontaneous emission will differ, we still expect qualitatively correct results for the spectral positions in which the PL exhibits local maxima, as both mechanisms are governed by the partial local density of states of the structure. Reflection (R) and transmission (T) coefficients are calculated as a solution of the diffraction problems of plane waves on the studied structures. For this aim we use the mapped pseudospectral time-domain method (PSTD).[35,36]

Our results for normalized QD PL obtained with this approach are presented in Figure 3c. As a trend, we observe a red-shift of the PL maximum as the nanodisk diameter is increased from d = 425 to d = 525 nm. Initially, this red-shift is accompanied by a spectral narrowing as the resonances move closer together, which becomes most pronounced in the region of the spectral overlap. For larger nanodisk diameters the spectrum broadens again as the resonances move further apart. For the samples with d = 550−600 nm, when the separation between the electric and magnetic dipole mode becomes much larger than their spectral widths, more than one local maximum is observed. The local maxima positions follow the spectral mode positions of the electric and magnetic dipole modes, shown with blue and red markers in Figure 3c.

Next, in order to experimentally investigate the emission properties of the coupled system, we have performed micro-PL spectroscopy of our samples. The results of our measurements are displayed in Figure 4. Details of the measurement procedure are included in the Methods section. The shaded areas in Figure 4 show the measured reference spectrum of the QDs embedded in polystyrene. The experimental QD PL spectra collected from the coupled system are also plotted in Figure 4 for samples #1−6 (solid lines). The reference QD PL is repeated as a shading for each sample. It is immediately obvious that the QD PL spectral line shape is strongly modified by the presence of the silicon nanodisk arrays and that it shows a systematic dependence on the resonance positions. Furthermore, the trends for the PL line shape predicted by the numerical calculations are well reproduced: From sample #1 to sample #4 the spectral position of the PL maximum is systematically shifted toward longer wavelengths, which is accompanied by a reduction of the emission line width; the fwhm of the PL spectrum is reduced from approximately 160 nm for sample #1 and 130 nm for sample #2 to less than 100 nm for samples #3 and #4. Around the spectral overlap (#3,#4) of the electric and magnetic resonance of the silicon nanodisk, we indeed observe a single maximum, as predicted by our theory, despite the lack of clear resonance signature in the transmission profiles (Figure 2). When proceeding to sample #5, on the other hand, a pronounced spectral broadening of the PL is observed, which now covers a broad range of more than 200 nm. This broadening further increases for sample #6 as the resonances are shifted further apart. However, the experimental curves appear generally blurred out as compared to theoretical spectra, which we attribute not only to sample imperfections but also to the fact that our theoretical model is based on normal-incidence calculations while in experiment the PL is collected for a range of emission angles. Another factor contributing to the observed deviations is the approximation of the active layer containing discrete QDs by a homogeneous gain medium.

An interesting feature in the obtained experimental PL spectra is the occurrence of an additional sharp and strong PL

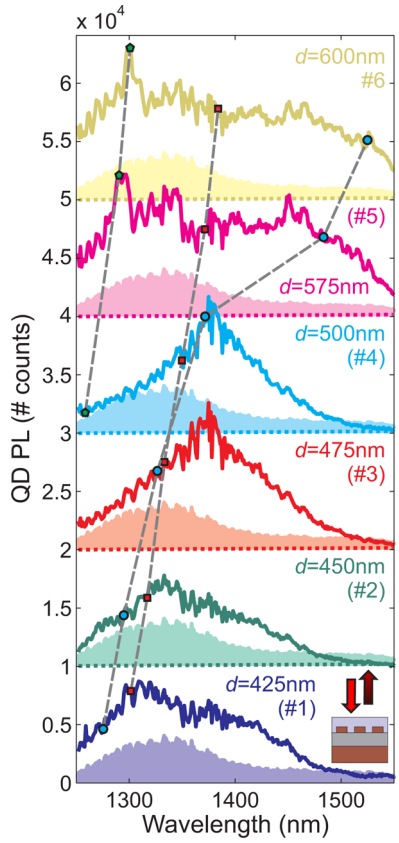

Figure 4. Measured QD photoluminescence spectra collected from the silicon nanodisk arrays with various nanodisk diameters in reflection geometry (see inset). PL spectra for different samples are vertically displaced by 10^4 counts for clarity. The reference QD PL is repeated as a shading in the corresponding color for each sample. The dashed gray lines and cyan, red, and green markers show the positions of the modes as indicated by the correspondingly colored solid lines in Figure 2a.

maximum at around 1300 nm wavelength for larger nanodisks; see for example sample #6 and the slightly blue-shifted feature for sample #5. The spectral positions of these additional maxima correspond well to those of the previously discussed higher-order modes observed in the experimental transmittance curves (see green line in Figure 2a). For these higher-order modes, the emission is enhanced only in a narrow region around their spectral positions, as clearly seen in Figure 4.

We note that, while in our work we experimentally observe a considerable increase of the PL intensity of the QDs coupled to all studied silicon nanodisks as compared to the PL collected from unstructured regions of the wafer (color shading adjacent to each spectrum), absolute values for PL enhancement cannot be derived from our experiment. In particular, the PL collected at the spectrometer can be affected by slight variations in the density of QDs in the polystyrene layer, and furthermore, the fraction of the total emitted power that can be collected by an objective with limited numerical aperture in reflection geometry (see Methods for details) will be influenced by possible directional effects. Indeed strong directional emission has been predicted for emitters coupled to silicon nanodisks.[16]

In conclusion, we have experimentally demonstrated that emission spectra of near-infrared emitting QDs can be shaped by coupling them to the electric and magnetic localized modes of subwavelength silicon nanodisk resonators. In particular, we

DOI: 10.1021/ph500379p
ACS Photonics 2015, 2, 172−177

have observed that for silicon nanodisks featuring different nanodisk diameters the PL spectral shape correlates with the resonance characteristics of the silicon nanodisks. In contrast to spectrally separate resonances, where the PL spectral shape can be predicted from the transmittance spectra, for silicon nanodisks with diameters corresponding to the condition of the overlap of the electric and magnetic resonance, the emission spectrum has a single maximum, despite the disappearance of the resonance characteristics in the transmission spectrum. Our results pinpoint that in the presence of electric and magnetic dipolar resonances a thorough undestanding of the underlying resonance properties of the all-dielectric nanoparticles is crucial in order to make predictions about the nanoparticles' influence on the radiation spectrum of emitters located in their vicinity. These findings have important implications for the design and optical characterization of all-dielectric nanoantennas with near-unity radiation efficiencies.

METHODS

Sample Fabrication. Silicon disks on silicon oxide were fabricated using electron-beam lithography (EBL) on silicon-on-insulator wafers (SOITEC, 220 nm top silicon thickness, 2 μm buried oxide thickness, backside polished) using the negative-tone resist NEB-31A. The resulting photoresist pattern was then used as an etch mask for reactive-ion etching. Remaining resist was removed by oxygen plasma. In the next step, PbS QDs (Evident, lot no. LNR-08-EPB, 10 mg/mL) were mixed with polystyrene (25 mg of polystyrene in 2.5 mL of toluene) in a 1:1 ratio. The mixture was spin-coated on top of the silicon nanodisk samples at 800 rpm for 10 s. This was repeated three times in order to obtain a film of approximately 250 nm thickness, resulting in the silicon disks being embedded inside the QD-PS matrix as schematically depicted in Figure 1. On the basis of the concentrations specified above, the QD density in the layer can be estimated to be on the order of 10^{17}QD/cm^3 after complete evaporation of the toluene.

Optical Transmittance Measurements. The linear-optical transmittance spectra of the fabricated samples were measured using a home-built setup, where the sample is back-side illuminated with an optical fiber brought into close proximity to the wafer back-side surface. Due to the large size of the fabricated silicon disk arrays (500 μm × 500 μm), no additional focusing was necessary in order to ensure all of the light is passing through the sample. The light transmitted through the sample was then collected on the other side of the sample using a Mitutoyo M Plan NIR 10× NA 0.26 objective and directed to a spectrometer (Acton Spectra Pro 2500i, 2 μm blazing) connected to a liquid-nitrogen-cooled InGaAs detector. Measurements were referenced to the transmittance of the sample next to the silicon nanodisk arrays. Transmittance values exceeding unity stem from Fabry−Perot resonances in the layered wafer structure in combination with the referencing procedure.

Microphotoluminescence Measurements. For micro-PL spectroscopy of our structures we excited the QDs by a pulsed laser (808 nm wavelength, 80 MHz repetition rate, 6.25 ns pulse length, 50 μW laser power) focused onto the sample with a Mitutoyo M Plan APO NIR HR 50× NA 0.65 objective. The same objective was used for collecting the PL in reflection configuration. A long-pass filter was introduced to remove the exciting laser light from the signal. The light emitted by the QDs was then directed through an optical fiber to the spectrometer (the same as used in the transmittance measurements). For each measurement we subtracted the dark counts and we corrected the final spectra with the instrument response characteristics.

ASSOCIATED CONTENT

Supporting Information

A detailed description of the gain model employed to obtain an estimate for the emission spectra of the coupled system. This material is available free of charge via the Internet at http://pubs.acs.org.

AUTHOR INFORMATION

Corresponding Author

*E-mail: isabelle.staude@anu.edu.au.

Notes

The authors declare no competing financial interest.

ACKNOWLEDGMENTS

We thank A. E. Miroshnichenko for useful discussion. This work was performed, in part, at the Center for Integrated Nanotechnologies, an Office of Science User Facility operated for the U.S. Department of Energy (DOE) Office of Science. Sandia National Laboratories is a multiprogram laboratory managed and operated by Sandia Corporation, a wholly owned subsidiary of Lockheed Martin Corporation, for the U.S. Department of Energy's National Nuclear Security Administration under contract DE-AC04-94AL85000. The authors also acknowledge support from the Australian Research Council through Centre of Excellence, Discovery Project, and DECRA Fellowship grants.

REFERENCES

(1) Novotny, L.; van Hulst, N. F. Antennas for light. *Nat. Photonics* **2011**, *5*, 83−90.
(2) Biagioni, P.; Huang, J.-S.; Hecht, B. Nanoantennas for visible and infrared radiation. *Rep. Prog. Phys.* **2012**, *75*, 024402.
(3) Wang, H.; Brandl, D. W.; Le, F.; Nordlander, P.; Halas, N. J. Nanorice: a hybrid plasmonic nanostructure. *Nano Lett.* **2006**, *6*, 827−832.
(4) Curto, A. G.; Volpe, G.; Taminiau, T. H.; Kreuzer, M. P.; Quidant, R.; van Hulst, N. F. Unidirectional emission of a quantum dot coupled to a nanoantenna. *Science* **2010**, *329*, 930−933.
(5) Staude, I.; Maksymov, I. S.; Decker, M.; Miroshnichenko, A. E.; Neshev, D. N.; Jagadish, C.; Kivshar, Yu. S. Broadband scattering by tapered nano-antennas. *Phys. Status Solidi RRL* **2012**, *6*, 466−468.
(6) Miroshnichenko, A. E.; Kivshar, Yu. S. Fano resonances in all-dielectric oligomers. *Nano Lett.* **2012**, *12*, 6459−6463.
(7) Chong, K. E.; Hopkins, B.; Staude, I.; Miroshnichenko, A. E.; Dominguez, J.; Decker, M.; Neshev, D. N.; Brener, I.; Kivshar, Yu. S. Observation of Fano resonances in all-dielectric nanoparticle oligomers. *Small* **2014**, *10*, 1985−1990.
(8) Liu, N.; Mukherjee, S.; Bao, K.; Li, Y.; Brown, L. V.; Nordlander, P.; Halas, N. J. Manipulating magnetic plasmon propagation in metallic nanocluster networks. *ACS Nano* **2012**, *6*, 5482−5488.
(9) Maksymov, I. S.; Miroshnichenko, A. E.; Kivshar, Yu. S. Plasmonic nanoantennas for efficient control of polarization-entangled photon pairs. *Phys. Rev. A* **2012**, *86*, 011801(R).
(10) Müller, M.; Bounouar, S.; Jöns, K. D.; Glässl, M.; Michler, P. On-demand generation of indistinguishable polarization-entangled photon pairs. *Nat. Photonics* **2014**, *8*, 224−227.
(11) Khurgin, J. B.; Sun, G.; Soref, R. A. Enhancement of luminescence efficiency using surface plasmon polaritons: figures of merit. *J. Opt. Soc. Am. B* **2007**, *24*, 1968−1980.
(12) Evlyukhin, A. B.; Novikov, S. M.; Zywietz, U.; Eriksen, R. L.; Reinhardt, C.; Bozhevolnyi, S. I.; Chichkov, B. N. Demonstration of

DOI: 10.1021/ph500379p
ACS Photonics 2015, 2, 172−177

magnetic dipole resonances of dielectric nanospheres in the visible region. *Nano Lett.* **2012**, *12*, 3749−3755.
(13) Kuznetsov, A. I.; Miroshnichenko, A. E.; Fu, Y. H.; Zhang, J.; Luk'yanchuk, B. Magnetic light. *Sci. Rep.* **2012**, *2*, 492.
(14) Ginn, J. C.; Brener, I.; Peters, D. W.; Wendt, J. R.; Stevens, J. O.; Hines, P. F.; Basilio, L. I.; Warne, L. K.; Ihlefeld, J. F.; Clem, P. G.; Sinclair, M. B. Realizing optical magnetism from dielectric metamaterials. *Phys. Rev. Lett.* **2012**, *108*, 097402.
(15) Person, S.; Jain, M.; Lapin, Z.; Sáenz, J. J.; Wicks, G.; Novotny, L. Demonstration of zero optical backscattering from single nanoparticles. *Nano Lett.* **2013**, *13*, 1806−1809.
(16) Staude, I.; Miroshnichenko, A. E.; Decker, M.; Fofang, N. T.; Liu, S.; Gonzales, E.; Dominguez, J.; Luk, T. S.; Neshev, D. N.; Brener, I.; Kivshar, Yu. S. Tailoring directional scattering through magnetic and electric resonances in subwavelength silicon nanodisks. *ACS Nano* **2013**, *7*, 7824−7832.
(17) Blanco, L. A.; García de Abajo, F. J. Spontaneous emission enhancement near nanoparticles. *J. Quant. Spectrosc. Radiat. Transfer* **2004**, *89*, 37−42.
(18) Sainidou, R.; Renger, J.; Teperik, T. V.; González, M. U.; Quidant, R.; García de Abajo, F. J. Extraordinary all-dielectric light enhancement over large volumes. *Nano Lett.* **2010**, *10*, 4450−4455.
(19) Pellegrini, G.; Mattei, G.; Mazzoldi, P. Light extraction with dielectric nanoantenna arrays. *ACS Nano* **2009**, *3*, 2715−2721.
(20) Khardikov, V. V.; Prosvirnin, S. L. Enhancement of the quantum dot luminescence in all-dielectric metamaterials. *Radio Phys. Radio Astron.* **2013**, *18*, 331−340.
(21) Devilez, A.; Stout, B.; Bonod, N. Compact metallo-dielectric optical antenna for ultra directional and enhanced radiative emission. *ACS Nano* **2010**, *4*, 3390−3396.
(22) Rolly, B.; Stout, B.; Bonod, N. Boosting the directivity of optical antennas with magnetic and electric dipolar resonant particles. *Opt. Express* **2012**, *20*, 20376−20386.
(23) Krasnok, A. E.; Miroshnichenko, A. E.; Belov, P. A.; Kivshar, Yu. S. All-dielectric optical nanoantennas. *Opt Exp.* **2012**, *20*, 20599−20604.
(24) Schmidt, M. K.; Esteban, R.; Sáenz, J. J.; Suárez-Lacalle, I.; Mackowski, S.; Aizpurua, J. Dielectric antennas - a suitable platform for controlling magnetic dipolar emission. *Opt. Express* **2012**, *20*, 13636−13650.
(25) Rolly, B.; Bebey, B.; Bidault, S.; Stout, B.; Bonod, N. Promoting magnetic dipolar transition in trivalent lanthanide ions with lossless Mie resonances. *Phys. Rev. B* **2012**, *85*, 245432.
(26) Biteen, J. S.; Lewis, N. S.; Atwater, H. A.; Mertens, H.; Polman, A. Spectral tuning of plasmon-enhanced silicon quantum dot luminescence. *Appl. Phys. Lett.* **2006**, *88*, 131109.
(27) Ringler, M.; Schwemer, A.; Wunderlich, M.; Nichtl, A.; Kürzinger, K.; Klar, T. A.; Feldmann, J. Shaping emission spectra of fluorescent molecules with single plasmonic nanoresonators. *Phys. Rev. Lett.* **2008**, *100*, 203002.
(28) Tanaka, K.; Plum, E.; Ou, J. Y.; Uchino, T.; Zheludev, N. I. Multifold enhancement of quantum dot luminescence in plasmonic metamaterials. *Phys. Rev. Lett.* **2010**, *105*, 227403.
(29) Decker, M.; Staude, I.; Shishkin, I.; Samusev, K.; Parkinson, P.; Sreenivasan, V. K. A.; Minovich, A.; Miroshnichenko, A. E.; Zvyagin, A.; Jagadish, C.; Neshev, D. N.; Kivshar, Yu. S. Dual channel spontaneous emission of quantum-dots in magnetic metamaterials. *Nat. Commun.* **2013**, *4*, 2949.
(30) Krishnamoorthy, H. N. S.; Jacob, Z.; Narimanov, E.; Kretzschmar, I.; Menon, V. M. Topological transitions in metamaterials. *Science* **2012**, *336*, 205−209.
(31) Rui, G.; Chen, W.; Abeysinghe, D. C.; Nelson, R. L.; Zhan, Q. Beaming circularly polarized photons from quantum dots coupled with plasmonic spiral antenna. *Opt. Express* **2012**, *20*, 19297−19304.
(32) Bermúdez Ureña, E.; Kreuzer, M. P.; Itzhakov, S.; Rigneault, H.; Quidant, R.; Oron, D.; Wenger, J. Excitation enhancement of a quantum dot coupled to a plasmonic antenna. *Adv. Mater.* **2012**, *24*, OP314−OP320.
(33) Habteyes, T. G.; Staude, I.; Chong, K. E.; Dominguez, J.; Decker, M.; Miroshnichenko, A. E.; Kivshar, Yu. S.; Brener, I. Near-field mapping of optical modes on all-dielectric silicon nanodisks. *ACS Photonics* **2014**, *1*, 794798.
(34) Decker, M.; Staude, I.; Falkner, M.; Dominguez, J.; Neshev, D. N.; Brener, I.; Pertsch, T.; Kivshar, Yu. S. High-efficiency light-wave control with all-dielectric optical Huygens' metasurfaces. *arXiv:1405.5038* [*physics.optics*], 2014.
(35) Gao, X.; Mirotznik, M. S.; Shi, S.; Prather, D. W. Applying a mapped pseudospectral time-domain method in simulating diffractive optical elements. *J. Opt. Soc. Am. A* **2004**, *21*, 777−785.
(36) Khardikov, V. V.; Iarko, E. O.; Prosvirnin, S. L. Using transmission matrix and pseudospectral time-domain method to study of light diffraction on planar periodic structures. *Radio Phys. Radio Astron.* **2008**, *13*, 146−158.

DOI: 10.1021/ph500379p
ACS Photonics 2015, 2, 172−177